

A Redundantly Actuated Ankle Rehabilitation Robot and Its Control Strategies

Mustafa Sinasi Ayas and Ismail Hakki Altas
Dep. of Electrical and Electronics Eng.
Karadeniz Technical University
61080, Trabzon, Turkey
msayas@ktu.edu.tr, ihaltens@ktu.edu.tr

Abstract—Robotic-based rehabilitation has attracted great attention since it provides various advantages from the viewpoint of patients, therapists and rehabilitation process. This paper presents a redundantly actuated ankle rehabilitation robot, its control schemes for the common rehabilitation exercises, and experimental results indicating the effectiveness of the control schemes and the performance of the controllers. In order to analyze the effect of external disturbance in position control scheme, the related experiments are performed with and without artificial disturbance required for making a fair performance comparison of the optimized controllers. The effectiveness of admittance control scheme is analyzed utilizing a healthy subject. The performance of the developed controllers are calculated using common performance indexes.

I. INTRODUCTION

Ankle sprain is one of the most common orthopedic injuries occurred in daily life [1], [2]. Traditional rehabilitation methods require physical therapists to rehabilitate patients one-to-one. The effectiveness of this rehabilitation process extremely depends on the therapist's skills. Since the rehabilitation process contains repetitive and intensive exercises, it can take a long time which affects the therapist in a negative way. Hence, the same therapist cannot deliver the same well rehabilitation process. Therefore, the importance and requirement of robotic-based rehabilitation has been emphasized by many studies from the viewpoint of patients, therapists and rehabilitation process [3]-[5].

Ankle rehabilitation robots provide various advantages such as:

- They provide a rich stream of measurement data to the therapists to record and observe every detail of the rehabilitation process and so make early alteration of the diagnosis, prognosis, and customization of possible therapy. In addition, therapists ensure about patients' compliance to the treatment regimens.
- They enable therapists to treat more patients by maximizing their free time.
- They accelerate patients' recovery by delivering more accurate, repetitive, intensive, and long enough therapies.

Ankle rehabilitation robots can be classified into two main categories as exoskeletons [4], [6], [7], i.e. wearable robots, and platform robots [8]-[14], although several design approaches have been proposed. Exoskeletons are not discussed

in this study, since only the devices used to manipulate ankles in sprained ankle treatment process are considered.

The most popular and earliest ankle rehabilitation system is the Rutgers Ankle proposed by Girone *et al.* [8]. Both passive and active training of the sprained ankle could be performed using the Rutgers Ankle. Zhang *et al.* [9] developed a 1-degree of freedom (DOF) rehabilitation device to perform the passive range of motion (ROM) exercises. A 3-SPS/SP parallel ankle rehabilitation robot was developed by Dai *et al.* [10]. Liu *et al.* [11] developed a parallel rehabilitation robot to perform plantarflexion/dorsiflexion, inversion/eversion, and abduction/adduction exercises. A parallel mechanism that could be used as a ROM exercise device and a balance/proprioception device was developed by Yoon *et al.* [12]. A redundantly actuated parallel robot with a central strut was proposed by Saglia *et al.* [13], [14].

In these aforementioned studies, authors neither revealed their controller performances using any specified performance index, nor used any optimization methods to tune the controller parameters in order to improve the controller performances. However, these developed devices contain one or more control type and thereby controllers such as position, velocity, torque, force, admittance, assistive, and resistive. In addition, control frameworks of the developed devices required for the most rehabilitation exercises anticipated by rehabilitation protocols were not clearly provided except [14].

The main purpose of this study is to present a developed 2-DOF redundantly actuated parallel ankle rehabilitation robot with its control framework. In addition, a proportional-integral-derivative (PID) controller and a fuzzy logic controller (FLC) both of which are optimized using Cuckoo search algorithm (CSA) for position control are introduced. Although we proposed an optimized PID controller [15] and an optimized FLC [16] for such a parallel rehabilitation robot in our previous studies, none of them present the control framework and also both of them performed in simulation environment. Furthermore, we also proposed a fractional order PID controller in our previous study [17] which does not cover the control framework presented in this study. In order to estimate the controller performances, error-based performance measurement methods, i.e. integral of absolute error (IAE), integral of time-weighted absolute error (ITAE), and integral

TABLE I: Range of motion for the human ankle [20]-[21]

| Motion type | Range |
|-----------------|---------|
| Dorsiflexion | 25°-30° |
| Plantar flexion | 40°-60° |
| Inversion | 20°-30° |
| Eversion | 10°-20° |

TABLE II: Ankle rehabilitation exercises

| Type of Exercise | Exercises | Mode |
|------------------|--|------------------|
| ROM | Dorsiflexion, Plantar flexion Inversion, Eversion | Passive & Active |
| Strengthening | Isometric, Isotonic | Active |

of squared error (ISE), are used. The controller performances when the ankle rehabilitation robot subject to external disturbance are also observed since the interaction between patient and robot results in disturbance effect. Furthermore, admittance control scheme of the robot required for providing assistance or resistance to the patient in strengthening exercises is presented in this study. It should be noted that neither [15] and [16] nor [17] proposed an admittance control scheme.

The rest of the paper is organized as follows. Section II presents a brief background about the developed 2-DOF redundantly actuated parallel ankle rehabilitation robot, and its inverse kinematic analysis. In Section III, the control strategies for rehabilitation exercises are introduced. The experimental setup used in this study and experimental results are given in Section IV. Finally, the conclusions are drawn.

II. ANKLE REHABILITATION ROBOT

A. Specifications

Anatomic structure of the human ankle is required in addition to the knowledge of the common ankle rehabilitation protocols in order to develop an ankle rehabilitation robot. The human ankle is capable of performing three kinds of movements, i.e. plantarflexion/dorsiflexion, inversion/eversion, and adduction/abduction movements through the ankle joint and subtalar joint in sagittal, frontal and transverse planes, respectively [18]. However, most of the ankle rehabilitation exercises are performed in frontal and sagittal planes [19], [20]. The ranges of motions for the human ankle given in Table I vary according to human age, gender, and left-right ankle [21].

The commonly used exercises in ankle rehabilitation are given in Table II. Plantar flexion/dorsiflexion and inversion/eversion movements are the common movements used as the range of motion (ROM) exercises, and isometric and isotonic exercises are the common strengthening exercises in ankle rehabilitation protocol. The patient does not apply any force/torque in passive mode exercises, while a force/torque is applied in active mode exercises. In order to perform these exercises a mechanism having at least 2-DOFs mobility is required with both position and admittance control schemes. It is important to note that the mechanism should provide the required range for each motion. For this purpose, a parallel mechanism shown in Fig. 1 is developed.



Fig. 1: The developed parallel ankle rehabilitation robot (a: Ankle connection platform; b: Force sensors; c: Moving platform; d: Central strut; e: Linear actuators; f: Base platform).

B. Description

The developed mechanism shown in Fig. 1 consists of a motionless base platform and a moving platform connected by 3 extensible legs and 1 strut located at the center. The 3 extensible legs consisting of DC electrical actuators (Concentric LACT4P-12V-5) are used to rotate the upper platform. The legs have a universal joint at the bottom end and a spherical joint at the upper end. The central strut with a universal joint at the bottom end and a spherical joint at the upper end supports the upper platform and limits the mobility of the device to 2 DOFs by fastening both moving and base platforms. As a result of the given design features a redundantly actuated mechanism which has high stiffness capability and singularity-free workspace [22] is developed.

C. Inverse Kinematic Analysis

The desired trajectory of the moving platform can be transformed in terms of the required lengths of each DC electrical actuator using inverse kinematic analysis of the mechanism. By controlling the position of the actuators, the desired length of each actuator can be achieved. Fig. 2 depicts the modeled parallel mechanism used in inverse kinematic analysis.

$O(x, y, z)$ and $C(u, v, w)$ are two different Cartesian coordinate systems located at the center of base and moving platforms, respectively. Two rotation angles α and β around u and v axes are shown in Fig. 2. The rotation matrix which expresses the orientation of the moving platform with reference to the base platform can be defined as in (1):

$${}^A R_B = R_v(\beta)R_u(\alpha) \quad (1)$$

where $R_v(\beta)$ and $R_u(\alpha)$ are given in (2) and (3), respectively.

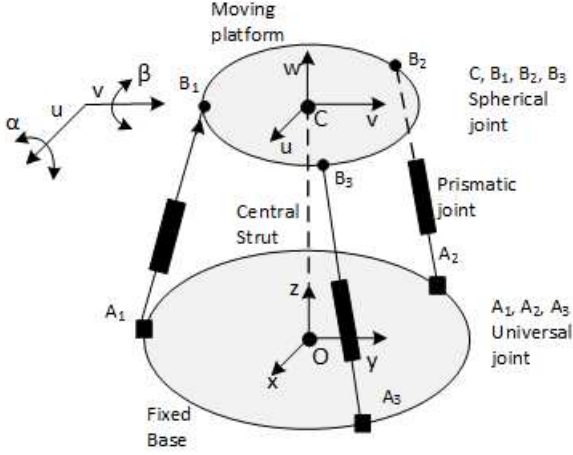


Fig. 2: The modeled mechanism.

$$R_v(\beta) = \begin{bmatrix} \cos(\beta) & 0 & \sin(\beta) \\ 0 & 1 & 0 \\ \sin(\beta) & 0 & \cos(\beta) \end{bmatrix} \quad (2)$$

$$R_u(\alpha) = \begin{bmatrix} 1 & 0 & 0 \\ 0 & \cos(\alpha) & -\sin(\alpha) \\ 0 & \sin(\alpha) & \cos(\alpha) \end{bmatrix} \quad (3)$$

A $X_p = [0, 0, p_z, \alpha, \beta, 0]^T$ vector consists of both position vector, \mathbf{p} , and orientation angles. The position vector $\mathbf{p} = [0, 0, p_z]^T$ is constant owing to the central strut.

The length of the i^{th} leg of the mechanism can be calculated as:

$$\overline{A_i B_i} = \mathbf{p} + {}^A R_B \mathbf{b}_i - \mathbf{a}_i, \quad i = 1, 2, 3 \quad (4)$$

where $\overline{A_i B_i}$ is the length of the i^{th} leg, $\mathbf{a}_i = [a_{ix}, a_{iy}, a_{iz}]^T$ is the position vector of A_i , and $\mathbf{b}_i = [b_{iu}, b_{iv}, b_{iw}]^T$ is the position vector of B_i .

III. CONTROL SCHEMES FOR REHABILITATION EXERCISES

The required control schemes for the ankle rehabilitation exercises are given in Table III. Position and admittance control are sufficient to achieve the particular exercises in both passive and active mode. It is clear that admittance control is only required in active mode, while position control is required for both of the modes.

When the mentioned exercises are considered:

- The passive ROM exercises in which the ankles are moved carefully by the rehabilitation robot are used when the patients can scarcely move their ankles. In order to achieve this movement along a certain trajectory at a steady speed, a position control scheme is required.
- The active ROM exercises are needed to fully recover the patients' ROM. In these exercises, the patients apply mild force to the moving platform of the rehabilitation robot to initiate the motion. Since they cannot provide sufficient force to complete the exercises, the robot should

TABLE III: Control types for ankle rehabilitation exercises

| Type of Exercise | Exercise/Mode | Type of Control |
|------------------|---------------|-----------------|
| ROM | Passive | Position |
| | Active | Admittance |
| Strengthening | Isometric | Active |
| | Isotonic | Active |
| | | Admittance |

assist them by observing their intentions by means of the force sensors located under the moving platform. An admittance control scheme is required to provide additional effort.

- Isometric exercises in which the moving platform is fixed to a certain position and then the patients apply force to it are also required a position control scheme to move the platform to desired fixed position. The applied force is monitored through the force sensors to comment the rehabilitation progress.
- Isotonic exercises which are one of the strengthening exercises are required an admittance control scheme to provide a certain resistance to the patient while moving the platform.

A. Position Control Scheme

Position control scheme is required for both passive and active exercises. Depending on the exercise, a reference trajectory/position defined by therapist has to be tracked/hold accurately. Fig. 3, where $l_i, i = 1, 2, 3$ is the length of i^{th} actuator corresponding to i^{th} leg, and X is the position vector containing orientation angles, shows the block diagram of the position control scheme. Required reference trajectory/position transformed in terms of required lengths of each actuator, i.e. l_i , by using inverse kinematic analysis. In order to obtain accurate reference tracking, the parameters of the designed PID controller and FLC are tuned using CSA. The optimization process were given in our previous simulation studies, [15], [16] where particle swarm optimization algorithm was used instead of CSA. It should be noted that the studies [15], [16] were performed in simulation environment, whereas this study was performed in real time. Optimized controller, i.e. PID controller or FLC, generates control signal $u_i, i = 1, 2, 3$ for i^{th} actuator driver.

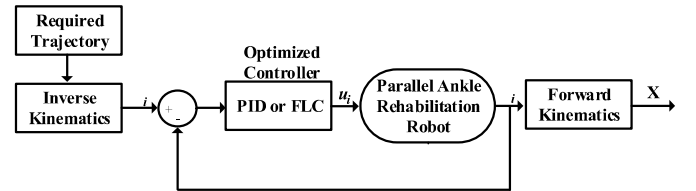


Fig. 3: Block diagram of position control scheme.

The performance of the controllers in position control scheme is measured using the ITAE, IAE and ISE performance indexes. The equations of the mentioned performance indexes are:

$$ITAE = \int_0^t t |e(t)| dt \quad (5)$$

$$IAE = \int_0^t |e(t)| dt \quad (6)$$

$$ISE = \int_0^t e(t)^2 dt \quad (7)$$

where $e(t)$ is the error between reference and actual signal.

B. Admittance Control Scheme

Active ROM exercises used for fully recover the patients' ROM, and strengthening exercises such as isotonic exercises are based on admittance control scheme. The relation between patient and robot can be introduced as a spring-damper model shown in Fig. 4, where f , x_r , k , and b are the applied force by the patient, reference position, spring and damping parameters, respectively. By measuring the applied force by the patient, the reference position x_r is estimated with an admittance filter given in (8).

$$x_r = \frac{f}{bs + k} \quad (8)$$

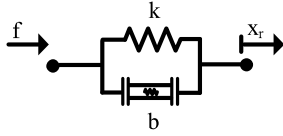


Fig. 4: Force-motion model.

Fig. 5 shows the block diagram of the admittance control scheme. The applied force is measured by means of three force sensors located under the moving platform seen in Fig. 1.

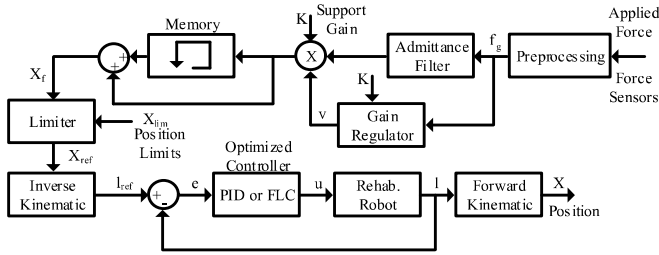


Fig. 5: Block diagram of admittance control scheme.

The reference position $X_{ref,i}$, $i = 1, 2, 3$ is estimated as in (10), where f_g , K , and $v(f_g, K)$ are preprocessed applied force, support gain and output of gain regulator, respectively. $Kv(f_g, K)$ value determines the level of assistance ($Kv(f_g, K) \geq 1$) or resistance ($Kv(f_g, K) < 1$). The higher $Kv(f_g, K)$ value for $Kv(f_g, K) \geq 1$ provides the higher support, i.e. higher assistance, while the lower $Kv(f_g, K)$ value for $Kv(f_g, K) < 1$ provides the higher resistance. $v(f_g, K)$ is based on fuzzy logic and calculates a scalar value to regulate the level of support. Fuzzy logic based gain regulator consist of fuzzification, rule table, inference system and defuzzification parts. The details of these parts

are not presented in this paper, since this study focuses on the general presentation of the developed rehabilitation robot and its control strategies.

$$X_{f,k} = X_{f,k-1} + Kv(f_g, K) \frac{f_g}{bs + k} \quad (9)$$

where k represents time instance.

$$X_{ref} = \begin{cases} X_f, X_{ref} < X_{lim} \\ X_{lim}, X_{ref} \geq X_{lim} \end{cases} \quad (10)$$

IV. EXPERIMENTAL RESULTS

Plantar flexion/dorsiflexion movement was performed in both passive and active mode. Two different experiments were performed in passive mode to compare the performance of both the PID controller and FLC, while one experiment was performed in active mode to indicate the effectiveness of the admittance control scheme. The experimental set up shown in Fig. 6 consists of six main elements: ankle rehabilitation robot, PC, power supply, data acquisition card (National Instruments, NI PCIe-6361), actuator driver, and force sensor amplifier board.

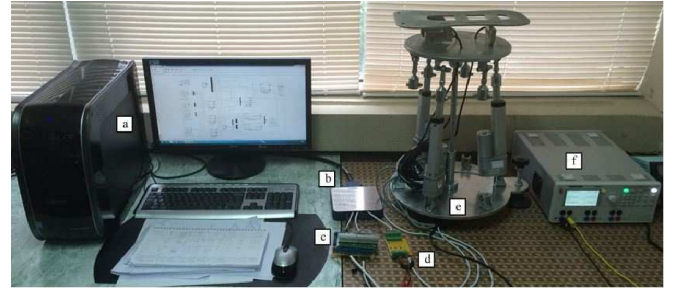


Fig. 6: Experimental set up (a: PC, b: Data acquisition card, c: Actuator driver, d: Force sensor amplifier board, e: Ankle rehabilitation robot, f: Power supply).

A sine signal with the frequency of 0.25 Hz was selected as the reference signal in the passive mode experiments. It should be noted that according to the specified reference trajectory, the required trajectory for each actuator was calculated using inverse kinematics in the experiments and the trajectory tracking control of each actuator was performed separately. Hence, tracking control results of each actuator entitled actuator#1, actuator#2, and actuator#3 were separately analyzed in the experiments. However, only the tracking responses and tracking errors for the actuator#1 are given as figure, since the results obtained for other actuators were nearly the same. The only difference of the experiments was that the first experiment was performed without any artificial disturbance, while the external disturbance was subjected to the system as payload in the second experiment. As the external disturbance, a known weight was put upon the ankle rehabilitation robot and retaken at the specific time intervals.

The tracking responses obtained in the first passive mode experiment using the PID controller and FLC are compared in Fig. 7, for the actuator#1. In addition, trajectory tracking errors for the actuator#1 are illustrated in Fig. 8. The

superiority of the FLC over the PID controller in transient and steady-state performance was deduced from the zoomed sections of the figures and tracking error figure. Performance results of the controllers required as small as possible for the first passive mode experiment are given in Table IV. The performance values of the FLC are smaller than those of the PID controller.

In the second passive mode ROM exercise, a known weight was put upon the ankle rehabilitation robot and retaken at the specific time intervals to change the available payload of the robot. The signals of the applied external disturbance for each actuator are given in Fig. 9. The obtained tracking responses for both controllers are given in Fig. 10. Trajectory tracking errors for the actuator#1 illustrated in Fig. 11 indicates that the FLC is superior to the PID controller even the external disturbance. Performance results of the controllers obtained in the second experiment are given in Table IV. It can be clearly inferred from the tracking error figures and performance results of the controllers given in Table IV that the FLC is better than the PID controller in terms of attenuating the external disturbance. The designed FLC has also better performance than fractional order PID controller designed in [17] which is our previous study.

Since tracking responses for the actuator#2 and actuator#3 resulted in similar trend with actuator#1, trajectory tracking responses and errors of these actuators were not demonstrated. However, performance results of the controllers for all actuators were given in Table IV.

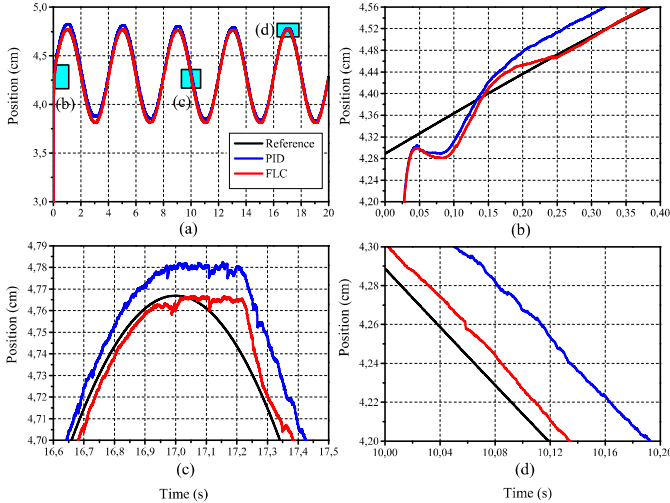


Fig. 7: Tracking response of actuator#1 in the first passive mode experiment.

In addition to the passive ROM exercises, an active ROM exercise using a healthy subject was also performed. It was asked to the subject to perform plantar flexion/dorsiflexion movement between -20 and 20 degrees by applying minimum possible force, since additional support was provided by the robot. The applied force by the subject and obtained platform orientation are given in Fig. 12, where the region *a* shows the relation between applied force and platform velocity. The more

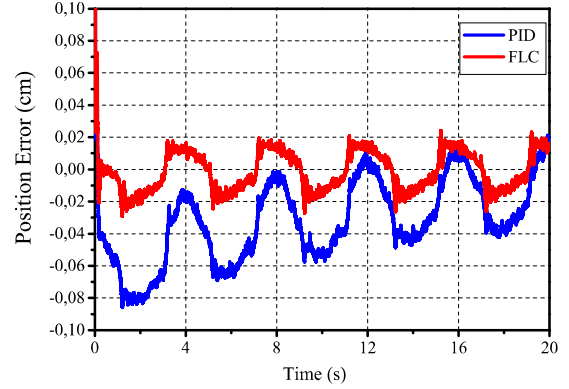


Fig. 8: Tracking error of actuator#1 in the first passive mode experiment.

applied force increased the velocity of the platform. Platform orientation was also limited between -20 and 20 degrees.

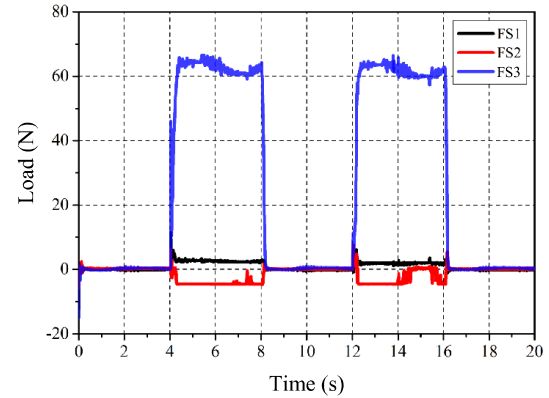


Fig. 9: Signals applied as external disturbance (FS: Force sensor).

V. CONCLUSION

A redundantly actuated ankle rehabilitation robot was presented and its control strategies for the common rehabilitation exercises were discussed in this study. Two kind of exercises, i.e. passive and active ROM exercises, were performed in the study. First, passive mode exercises were performed as two different experiments in order to show the performances of both the FLC and PID controller. The design and optimization process of the controllers were performed using the same structure except the optimization algorithm in the previous simulation studies [15], [16]. It was inferred that the FLC is better than the PID controller in terms of attenuating the external disturbance and tracking performance. Then, an active ROM exercise was performed and the effectiveness of the admittance control scheme was observed.

ACKNOWLEDGMENT

This work was supported by Scientific and Technological Research Council of Turkey (TUBITAK), Project No.

TABLE IV: Performance results of the controllers obtained in the passive mode experiments

| | | Actuator#1 | | | Actuator#2 | | | Actuator#3 | | |
|--------------------------|-----|------------|--------|--------|------------|--------|--------|------------|--------|--------|
| | | IAE | ISE | ITAE | IAE | ISE | ITAE | IAE | ISE | ITAE |
| 1st Exp. (No dist.) | PID | 0.7204 | 0.1166 | 5.3448 | 0.7562 | 0.1207 | 5.7543 | 0.8156 | 0.1287 | 6.6800 |
| | FLC | 0.2580 | 0.0864 | 2.1950 | 0.2838 | 0.0870 | 2.4696 | 0.3674 | 0.0918 | 3.2508 |
| 2nd Exp. (With dist.) | PID | 0.8509 | 0.1368 | 6.7987 | 0.8314 | 0.1290 | 6.6999 | 1.1235 | 0.1686 | 9.9514 |
| | FLC | 0.3407 | 0.0964 | 2.8968 | 0.3484 | 0.0880 | 3.1883 | 0.5378 | 0.0979 | 5.0717 |

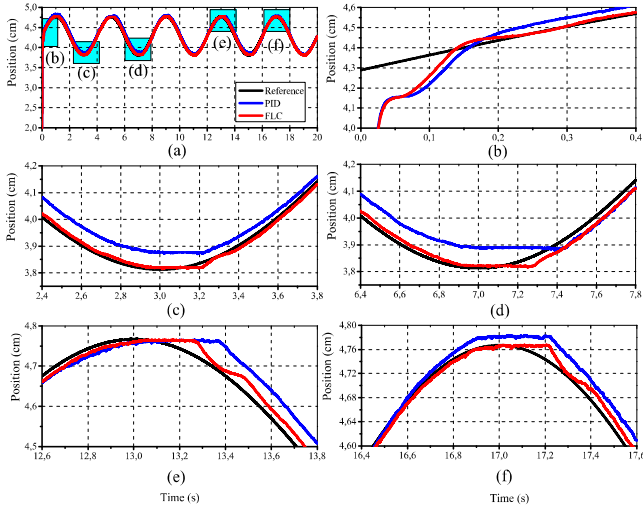


Fig. 10: Tracking response of actuator#1 in the second passive mode experiment.

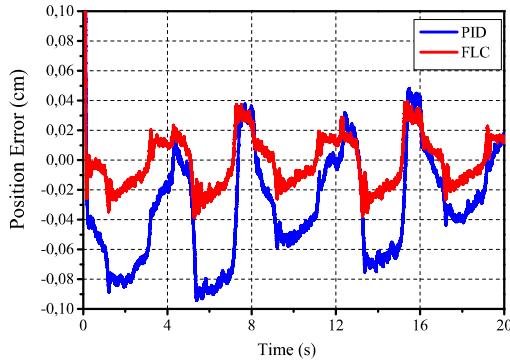


Fig. 11: Tracking error of actuator#1 in the second passive mode experiment.

114E025.

REFERENCES

- [1] E. Kemler, I. Port, H. Valkenberg, A. Hoes, and F. Backx, "Ankle injuries in the netherlands: Trends over 10–25 years," *Scandinavian journal of medicine & science in sports*, vol. 25, no. 3, pp. 331–337, 2015.
- [2] T. Mittlmeier and A. Wichelhaus, "Subtalar joint instability," *European Journal of Trauma and Emergency Surgery*, vol. 41, no. 6, pp. 623–629, 2015.
- [3] J. A. Saglia, N. G. Tsagarakis, J. S. Dai, and D. G. Caldwell, "A high performance redundantly actuated parallel mechanism for ankle rehabilitation," *The International Journal of Robotics Research*, 2009.
- [4] P. K. Jamwal, S. Q. Xie, S. Hussain, and J. G. Parsons, "An adaptive wearable parallel robot for the treatment of ankle injuries," *Mechatronics, IEEE/ASME Transactions on*, vol. 19, no. 1, pp. 64–75, 2014.

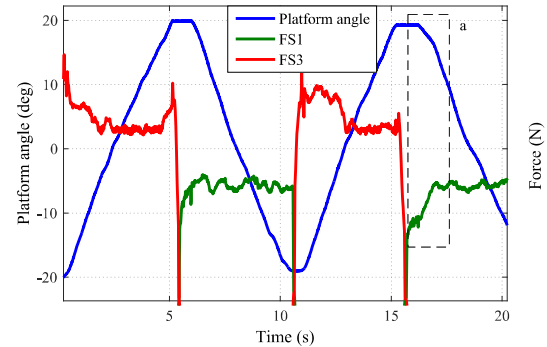


Fig. 12: Measured forces and obtained platform orientation in active ROM exercise.

- [5] C. Wang, L. Wang, J. Qin, Z. Wu, L. Duan, Z. Li, M. Cao, W. Li, Z. Lu, M. Li *et al.*, "Development of an ankle rehabilitation robot for ankle training," in *Information and Automation, 2015 IEEE International Conference on*. IEEE, 2015, pp. 94–99.
- [6] K. E. Gordon, G. S. Sawicki, and D. P. Ferris, "Mechanical performance of artificial pneumatic muscles to power an ankle-foot orthosis," *Journal of biomechanics*, vol. 39, no. 10, pp. 1832–1841, 2006.
- [7] A. Roy, H. I. Krebs, D. J. Williams, C. T. Bever, L. W. Forrester, R. M. Macko, and N. Hogan, "Robot-aided neurorehabilitation: a novel robot for ankle rehabilitation," *Robotics, IEEE Transactions on*, vol. 25, no. 3, pp. 569–582, 2009.
- [8] M. Girone, G. Burdea, and M. Bouzit, "The rutgers ankle orthopedic rehabilitation interface," *Proc. ASME Dyn. Syst. Control Div.*, vol. 67, pp. 305–312, 1999.
- [9] L.-Q. Zhang, S. G. Chung, Z. Bai, D. Xu, E. M. Van Rey, M. W. Rogers, M. E. Johnson, and E. J. Roth, "Intelligent stretching of ankle joints with contracture/spasticity," *Neural Systems and Rehabilitation Engineering, IEEE Transactions on*, vol. 10, no. 3, pp. 149–157, 2002.
- [10] J. S. Dai, T. Zhao, and C. Nester, "Sprained ankle physiotherapy based mechanism synthesis and stiffness analysis of a robotic rehabilitation device," *Autonomous Robots*, vol. 16, no. 2, pp. 207–218, 2004.
- [11] G. Liu, J. Gao, H. Yue, X. Zhang, and G. Lu, "Design and kinematics analysis of parallel robots for ankle rehabilitation," in *Intelligent Robots and Systems, 2006 IEEE/RSJ International Conference on*. IEEE, 2006, pp. 253–258.
- [12] J. Yoon, J. Ryu, and K.-B. Lim, "Reconfigurable ankle rehabilitation robot for various exercises," *Journal of Robotic Systems*, vol. 22, no. S1, pp. S15–S33, 2006.
- [13] J. Saglia, N. Tsagarakis, J. Dai, and D. Caldwell, "Inverse-kinematics-based control of a redundantly actuated platform for rehabilitation," *Proceedings of the Institution of Mechanical Engineers, Part I: Journal of Systems and Control Engineering*, vol. 223, no. 1, pp. 53–70, 2009.
- [14] J. Saglia, N. G. Tsagarakis, J. S. Dai, D. G. Caldwell *et al.*, "Control strategies for patient-assisted training using the ankle rehabilitation robot (arbot)," *Mechatronics, IEEE/ASME Transactions on*, vol. 18, no. 6, pp. 1799–1808, 2013.
- [15] M. S. Ayas, E. Sahin, and I. H. Altas, "Optimized control of a parallel mechanism rehabilitation robot," in *IASTED International Conference on Robotic Applications, Switzerland, DOI*, vol. 10, pp. 2014–817.
- [16] M. S. Ayas, I. H. Altas, and E. Sahin, "An optimized fuzzy logic controller for a parallel mechanism rehabilitation robot," in *Fuzzy*

Systems (FUZZ-IEEE), 2015 IEEE International Conference on. IEEE, 2015, pp. 1–6.

- [17] M. S. Ayas, I. H. Altas, and e. Sahin, “Fractional order based trajectory tracking control of an ankle rehabilitation robot,” *Transactions of the Institute of Measurement and Control*, p. 0142331216667810, 2016.
- [18] M. Dettwyler, A. Stacoff, I. A. Kramers-de Quervain, and E. Stüssi, “Modelling of the ankle joint complex. reflections with regards to ankle prostheses,” *Foot and ankle Surgery*, vol. 10, no. 3, pp. 109–119, 2004.
- [19] K. A. Payne, K. Berg, and R. W. Latin, “Ankle injuries and ankle strength, flexibility, and proprioception in college basketball players,” *Journal of athletic training*, vol. 32, no. 3, p. 221, 1997.
- [20] C. G. Mattacola and M. K. Dwyer, “Rehabilitation of the ankle after acute sprain or chronic instability,” *Journal of athletic training*, vol. 37, no. 4, p. 413, 2002.
- [21] H. Hallaceli, V. Uruc, H. H. Uysal, R. Ozden, C. Hallaceli, F. Soyuer, T. I. Parpucu, E. Yengil, and U. Cavlak, “Normal hip, knee and ankle range of motion in the turkish population,” *Acta orthopaedica et traumatologica turcica*, vol. 48, no. 1, pp. 37–42, 2014.
- [22] M. ValÁšek, V. Bauma, K. Belda, P. Plša *et al.*, “Design-by-optimization and control of redundantly actuated parallel kinematics sliding star,” *Multibody System Dynamics*, vol. 14, no. 3–4, pp. 251–267, 2005.